



ISSN: 0975-833X

Available online at <http://www.journalcra.com>

International Journal of Current Research
Vol. 9, Issue, 05, pp.51120-51123, May, 2017

INTERNATIONAL JOURNAL
OF CURRENT RESEARCH

RESEARCH ARTICLE

AUTOMATIC GLAUCOMA SCREENING USING SUPERPIXEL SEGMENTATION

*Manisha Kulkarni and Bhatlawande, V. S.

Dept. of E&TC, Siddhant College of Engineering, Sudumbare, Pune, India

ARTICLE INFO

Article History:

Received 24th February, 2017
Received in revised form
21st March, 2017
Accepted 04th April, 2017
Published online 31st May, 2017

Key words:

Glaucoma; CDR;
Superpixel Segmentation.

Copyright©2017, Manisha Kulkarni and Bhatlawande. This is an open access article distributed under the Creative Commons Attribution License, which permits unrestricted use, distribution, and reproduction in any medium, provided the original work is properly cited.

Citation: Manisha Kulkarni and Bhatlawande, V. S. 2017. "Automatic glaucoma screening using superpixel segmentation", *International Journal of Current Research*, 9, (05), 51120-51123.

ABSTRACT

Glaucoma is the second leading cause of loss of vision in the world. Currently, there is no effective method for simple, accurate and low cost glaucoma detection or screening. Automatic optic nerve head assessment from 2D retinal fundus images is promising for low cost glaucoma screening. This paper presents efficient method for cup to disc ratio (CDR) assessment using 2D retinal fundus images. The disc segmentation is carried out using active shape model (ASM), elliptical hough transform (EHT) and superpixel segmentation techniques. Among these three methods, one best output depending upon self assessment confidence score is considered for further processing. Cup to disc (CDR) ratio is calculated for the assessment of glaucoma. Based on performance of each method superpixel method performs best and more reliable.

INTRODUCTION

Glaucoma is a group of eye diseases which result in damage to the optic nerve and vision loss. About 6 to 67 million people have glaucoma globally and it is the second-leading cause of blindness after cataracts (Aquino, 2010 and Hoover, 2003). It occurs more commonly among older people. Glaucoma is classified in to open-angle glaucoma, closed-angle glaucoma and normal-tension glaucoma (Rovira, 2008). Open angle glaucoma develops slowly over time and there is no pain. Side vision may begin to decrease followed by central vision resulting in blindness if not treated. Closed-angle glaucoma can present gradually or suddenly (Aquino, 2010). Glaucoma results in to severe eye pain, blurred vision, mid-dilated pupil, redness of the eye, and permanent vision loss. Risk factors for glaucoma include increased pressure above 21mmHg or 2.8 kPa in the eye, a family history of the condition, migraines, high blood pressure, and obesity (Hoover, 2003 and Rovira, 2008). The paper is organized with six sections: The first section is an introduction including previous research on glaucoma detection. Second section refers to superpixel segmentation followed by third section EHT. Section four elaborates the experimental results. Final section concludes the work.

Superpixel segmentation

Superpixels captures redundancy of intensity value to compute local image features for the segmentation.

*Corresponding author: Manisha Kulkarni

Dept. of E&TC, Siddhant College of Engineering, Sudumbare, Pune, India

Superpixel image segmentation is faster, easy to use, and produce high quality segmentation. As we will demonstrate, they often suffer from a high computational cost, poor quality segmentation, inconsistent size and shape, or contain multiple difficult-to-tune parameters. Superpixel segmentation technique is widely used for object class recognition and medical image segmentation because of its simplicity and greater performance at a lower computational cost in comparison to existing methods. We have used simple linear iterative clustering (SLIC) algorithm to perform a local clustering of pixels in the 5-D space defined by the L, a, b values of the CIELAB color space and the x, y pixel coordinates. A novel distance measure enforces compactness and regularity in the superpixel shapes, and seamlessly accomodates grayscale as well as color images. SLIC generates superpixels by clustering pixels based on their color similarity and proximity in the image plane which can be done by five-dimensional [labxy] space, where [lab] is the pixel color vector in CIELAB color space, which is widely considered as perceptually uniform for small color distances, and xy is the pixel position. For an image with N pixels, the approximate size of each superpixel is therefore N/K pixels, where K is total number of superpixels. For roughly equally sized superpixels there would be a superpixel center at every grid interval $S = p N/K$. At the onset of our algorithm, we choose K superpixel cluster centers $C_k = [l_k, a_k, b_k, x_k, y_k]^T$ with $k = [1, K]$ at regular grid intervals S. Since the spatial extent of any superpixel is approximately S^2 (the approximate area of a superpixel), we can safely assume that pixels that are associated with this cluster center lie within a $2S \times 2S$ area around the superpixel center on the xy plane.

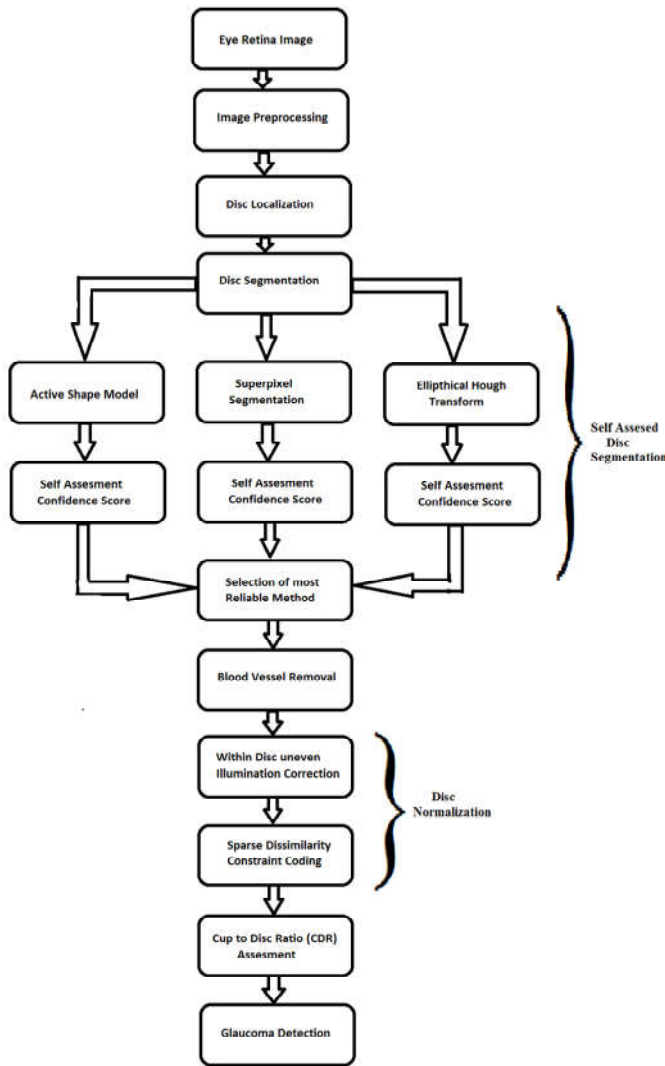


Fig. 1. Block diagram of Glaucoma screening system

This becomes the search area for the pixels nearest to each cluster center. Euclidean distances in CIELAB color space are perceptually meaningful for small distances (Eq. 1). If spatial pixel distances exceed this perceptual color distance limit, then they begin to outweigh pixel color similarities (resulting in superpixels that do not respect region boundaries, only proximity in the image plane). Therefore, instead of using a simple Euclidean norm in the 5D space, we use a distance measure D_s defined as follows:

$$d_{lab} = \sqrt{(l_k - l_i)^2 + (a_k - a_i)^2 + (b_k - b_i)^2} \dots\dots\dots(1)$$

$$d_{xy} = \sqrt{(x_k - x_i)^2 + (y_k - y_i)^2} \dots\dots\dots(2)$$

$$D_s = d_{lab} + \frac{m}{s} \cdot d_{xy}$$

$$D_s = d_{lab} + (m/s)d_{xy} = d_{lab} + \frac{m}{s} \cdot d_{xy} \dots\dots\dots(3)$$

where D_s is the sum of the L^*a^*b distance and the xy plane distance normalized by the grid interval S . A variable m is introduced in D_s allowing us to control the compactness of a superpixel. The greater the value of m , the more spatial proximity is emphasized and the more compact the cluster. This value can be in the range (Aquino, 2010 and Abr`amoff, 2009). We choose $m = 10$ for all the results in this paper. This roughly matches the empirical maximum perceptually

meaningful CIELAB distance and offers a good balance between color similarity and spatial proximity. SLIC begin by sampling K regularly spaced cluster centers and moving them to seed locations corresponding to the lowest gradient position in a 3×3 neighborhood. This is done to avoid placing them at an edge and to reduce the chances of choosing a noisy pixel. Image gradients are computed as:

$$G(x, y) = \|I(x + 1, y) - I(x - 1, y)\|^2 + \|I(x, y + 1) - I(x, y - 1)\|^2 \dots\dots\dots(4)$$

where $I(x, y)$ is the lab vector corresponding to the pixel at position (x, y) , and $\| \cdot \|$ is the L2 norm. This takes into account both color and intensity information. Each pixel in the image is associated with the nearest cluster center whose search area overlaps this pixel. After all the pixels are associated with the nearest cluster center, a new center is computed as the average labxy vector of all the pixels belonging to the cluster. We then iteratively repeat the process of associating pixels with the nearest cluster center and recomputing the cluster center until convergence. At the end of this process, a few stray labels may remain, that is, a few pixels in the vicinity of a larger segment having the same label but not connected to it. While it is rare, this may arise despite the spatial proximity measure since our clustering does not explicitly enforce connectivity. Nevertheless, we enforce connectivity in the last step of our algorithm by relabeling disjoint segments with the labels of the largest neighboring cluster.

Elliptical hough transform

The Hough Transform is an algorithm presented by Paul Hough in 1962 for the detection of features of a particular shape like lines or circles in digitalized images. In its classical form it was restricted to features that can be described in a parametric form. However, a generalized version of the algorithm exists which can also be applied to features with no simple analytic form, but it is very complex in terms of computation time. Hough transform can be applied to many computer vision problems as most images contain feature boundaries which can be described by regular curves. The main advantage of the Hough transform technique is that it is tolerant of gaps in feature boundary descriptions and is relatively unaffected by image noise, unlike edge detectors. One important difference between the Hough transform and other approaches is resistance of the former to noise in the image and its tolerance towards holes in the boundary line.

The strategy is to first construct the ellipse center from the tangent directions of a number of edge points, making use of the geometry of an ellipse. An ellipse can be represented in parametric form as:

$$x(\theta) = a_0 + a_x \cdot \sin(\theta) + b_x \cdot \cos(\theta) \quad y(\theta) = b_0 + a_y \cdot \sin(\theta) + b_y \cdot \cos(\theta) \dots\dots\dots(4)$$

Where (a_0, b_0) is the center of the ellipse and (a_x, a_y) and (b_x, b_y) are vectors representing the major and minor axes of the ellipse.

EXPERIMENTAL RESULTS

Experiments are performed on DRINOS & STARE database (Bock, 2010). The performance of algorithm is evaluated on

the basis of overlapping error and CDR error. The overlapping error E is computed as one evaluation metric to examine the difference between automated and manual cup: $E = 1 - (\text{Area}(S \cap M) / \text{Area}(\text{SUM}))$, where S and M denote the segmented and the manual cup respectively.

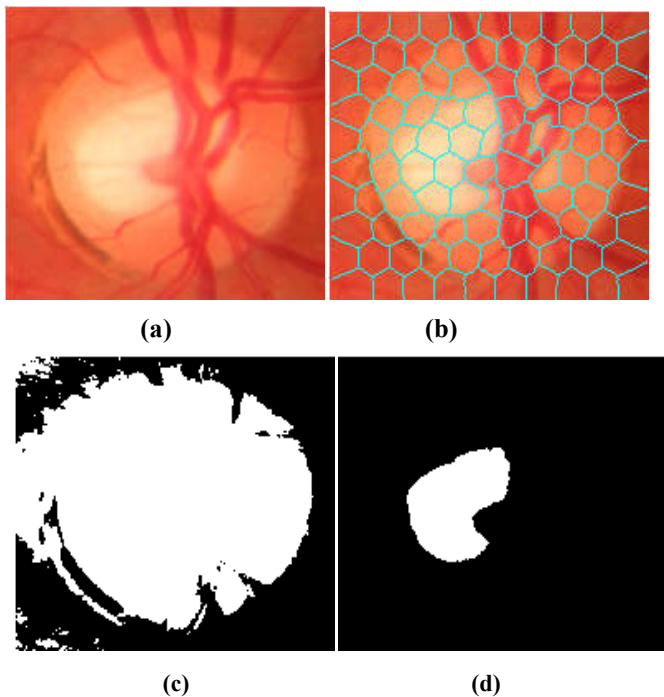


Fig. 2 a) original retinal image b) superpixel segmentation c) disc segmentation d) cup segmentation

In addition, the CDR accuracy is also evaluated using CDR error, computed as $\delta = |\text{CDR}_m - \text{CDR}|$, where CDR_m denotes the manual CDR

Conclusion

In this paper, we have presented a superpixel classification based cup segmentation for glaucoma detection. The location information further improves the results as it incorporates the prior knowledge of the cup. The accuracy of our current method is much better than previous methods. The glaucoma detection accuracy by the proposed method is only slightly below the manual CDR. From the discussions with clinicians, it is good enough for a large-scale glaucoma screening program. However, there are still many aspects for improvement in the proposed methods. For example, the proposed method under-estimates the very large cups while over-estimating the very small cups when pallor is very weak or absent. In addition, CDR based screening also has its limitations. Therefore, combining CDR with other factors are expected to further improve the performance. In the future, we would explore the integration of other factors to improve diagnosis outcomes toward a more reliable and efficient glaucoma screening system.

REFERENCES

- Abr'amoff, M. D., Alward, W. L. M., Greenlee, L. Shuba, E. C., Kim, C. Y., Fingert, J. H. and Y. H. Kwon, "Automated segmentation of the optic disc from stereo color photographs using physiologically plausible features," *Invest. Ophthalmol. Vis. Sci.*, vol. 48, pp. 1665–1673, 2007.
- Abr'amoff, M. D., Garvin, M. K. and Sonka, M. 2010. "Retinal imaging and image analysis," *IEEE Trans. Med. Imag.*, vol. 3, pp. 169–208.
- Abr'amoff, M. D., K. Lee, M. Niemeijer, W. L. M. Alward, E. Greenlee, K. Garvin, M. Sonka, and Y. H. Kwon, "Automated segmentation of the cup and rim from spectral domain OCT of the optic nerve head," *Inv Ophthalmol Vis Sci.*, vol. 50, pp. 5778–5784, 2009.
- Aquino, A., Gegundez-Arias, M. and Marin, D. 2010. "Detecting the optic disc boundary in digital fundus images using morphological, edge detection, and feature extraction techniques," *IEEE Trans. Med. Imag.*, vol. 29, pp. 1860–1869.
- Bock, R. J. Meier, L. G. Nyl, and G. Michelson, "Glaucoma risk index: Automated glaucoma detection from color fundus images," *Med. Image Anal.*, vol. 14, pp. 471–481, 2010.
- Bock, R., Meier, J., Michelson, G., Nyl, L. G. and J. Hornegger, "Classifying glaucoma with image-based features from fundus photographs," *Proc. of DAGM*, pp. 355–364, 2007.
- Centre for Eye Research Australia, Tunnel vision : the economic impact of primary open angle glaucoma. [electronic resource], 2008, <http://nla.gov.au/nla.arc-86954>.
- Cheng, J., Liu, J., Wong, D. W. K., Yin, F., Cheung, C., Baskaran, M., Aung, T. and Wong, T. Y. 2011. "Automatic optic disc segmentation with peripapillary atrophy elimination," *Int. Conf. of IEEE Eng. in Med. and Bio. Soc.*, pp. 6624–6627.
- Cheng, J., Liu, J., Xu, Y. Yin, F. Wong, D. W. K., Tan, N. M. Tao, D. Y. Cheng, T. Aung, and T. Y. Wong, "Superpixel classification based optic disc and optic cup segmentation for glaucoma screening," *IEEE Trans. Med. Imaging*, vol. 32, pp. 1019–1032, 2013.
- Cheng, J., Liu, J., Xu, Y., Yin, F., Wong, D. W. K., Tan, N. M. Cheung, C. Y., Tham, Y. C., and Wong, T. Y. "Superpixel classification based optic disc segmentation," In: Lee, K. M., Matsushita, Y., Rehg, J. M., Hu, Z. (eds.) ACCV, Part II, LNCS, vol. 7725, pp. 293–304, 2013.
- Cheng, J., Liu, J., Yin, F., Lee, B. H., Wong, D. W. K., Aung, T., Cheng, C. Y. and Wong, T. Y. 2013. "Self-assessment for optic disc segmentation," *IEEE Int. Conf. Eng. in Med. and Bio. Soc.*, pp. 5861–5864.
- Damms and F. Dannheim, T. 1993. "Sensitivity and specificity of optic disc parameters in chronic glaucoma," *Invest. Ophthalm. Vis. Sci.*, vol. 34, pp. 2246–2250, 1993.
- Foracchia, M., Grisan, E. and A. Ruggeri, "Detection of optic disc in retinal images by means of a geometrical model of vessel structure," *IEEE Trans. Med. Imag.*, vol. 23, no. 10, pp. 1189–1195, 2004.
- Foster, P. J., Oen, F. T., Machin, D., Ng, T. P., J. G. Devereux, G. J. Johnson, P. T. Khaw, and S. K. Seah, 2000. "The prevalence of glaucoma in Chinese residents of Singapore: a cross-sectional population survey of the Tanjong Pagar district," *Arch. Ophthalmol.*, vol. 118(8), pp. 1105–1111, 2000.
- Harizman, N., C. Oliveira, A. Chiang, C. Tello, M. Marmor, R. Ritch, and J. M. Liebmann, "The isht rule and differentiation of normal from glaucomatous eyes," vol. 124, pp. 1579–1583, 2006.
- Hoover, A. and Goldbaum, M. 2003. "Locating the optic nerve in a retinal image using the fuzzy convergence of the blood vessels," *IEEE Trans. Med. Imag.*, vol. 22, pp. 951–958.

- Hu, Z. M. D. Abr'amoff, Y. H. Kwon, K. Lee, and M. K. Garvin, "Automated segmentation of neural canal opening and optic cup in 3-d spectral optical coherence tomography volumes of the optic nerve head," *Inv Ophthalmol Vis Sci.*, vol. 51, pp. 5708–5717, 2010.
- Joshi, G. D., Sivaswamy, J. and Krishnadas, S. R. 2011. "Optic disk and cup segmentation from monocular color retinal images for glaucoma assessment," *IEEE Trans. Med. Imag.*, vol. 30, pp. 1192–1205.
- Joshi, G. D., Sivaswamy, J., Karan, K. and Krishnadas, R. 2010. "Optic disk and cup boundary detection using regional information," in *Proc. IEEE Int. Symp. Biomed. Imag.*, pp. 948–951.
- Li, H. and Chutatape, O. 2001. "Automatic location of optic disc in retinal images," in *Proc. Int. Conf. Image Processing*, vol. 2, pp. 837–840.
- Li, H. and Chutatape, O. 2004. "Automated feature extraction in color retinal images by a model based approach," *IEEE Trans. Biomed. Eng.*, vol. 51, no. 2, pp. 246–254, Feb 2004.
- Meier, J. Bock, R. Michelson, G. Nyl, L. G. and Hornegger, J. 2007. "Effects of preprocessing eye fundus images on appearance based glaucoma classification," *Proc. CAIP*, pp. 165–172.
- Michael, D. and Hancox, O. D. 1999. "Optic disc size, an important consideration in the glaucoma evaluation," *Clinical Eye and Vision Care*, vol. 11, pp. 59–62, 1999.
- Quigley, H. A. and Broman, A. T. 2006. "The number of people with glaucoma worldwide in 2010 and 2020," *Br. J. Ophthalmol.*, vol. 90(3), pp. 262–267.
- Rovira, A. P. and Trucco, E. 2008. "Robust optic disc location via combination of weak detectors," in *Proc. Int. Conf. IEEE Eng. Med. Bio. Soc.*, pp. 3542–3545.
- Shen, S. Y., T. Y. Wong, P. J. Foster, J. L. Loo, M. Rosman, S. C. Loon, W. L. Wong, S. M. Saw, and T. Aung, "The prevalence and types of glaucoma in malay people: the singapore malay eye study," *Invest. Ophthalmol. Vis. Sci.*, vol. 49(9), pp. 3846–3851, 2008.
- Wang, J. Yang, J. Yu, K. Lv, F. Huang, T. and Gong, Y. 2010. "Locality-constrained linear coding for image classification," *IEEE Int. Conf. on computer vision and pattern recognition*, pp. 3360–3367.
- Xu, J., Chutatape, O., E. Sung, C. Zheng, and P.C.T. Kuan, "Optic disk feature extraction via modified deformable model technique for glaucoma analysis," *Pattern Recognition*, vol. 40, pp. 2063–2076, 2007.
- Xu, Y. S. Lin, D. W. K. Wong, J. Liu, and D. Xu, "Efficient reconstruction-based optic cup localization for glaucoma screening," In: Mori, K., Sakuma, I., Sato, Y., Barillot, C., Nassir, N.(eds.) *MICCAI 2013, Part III, LNCS*, vol. 8151, pp. 445–452, 2013.
- Yin, F., Liu, J., Ong, S. H., Sun, Y., Wong, D. W. K., Tan, N. M., Cheung, C., Baskaran, M., Aung, T. and Wong, T. Y. 2011. "Model-based optic nerve head segmentation on retinal fundus images," *Int. Conf. of IEEE Eng. in Med. and Bio. Soc.*, pp. 2626–2629.
- Yin, F., Liu, J., Wong, D. W. K., Tan, N. M., Cheung, C., Baskaran, M., Aung, and Wong, T. Y. 2012. "Automated segmentation of optic disc and optic cup in fundus images for glaucoma diagnosis," *IEEE Int. Symp. on Computer-Based Medical Systems*, pp. 1–6.
- Zhang, Z. B. H. Lee, J. Liu, D. W. K. Wong, N. M. TAN, J. H. Lim, F. S. Yin, W. M. Huang, and H. Li, "Optic disc region of interest localization in fundus image for glaucoma detection in argali," *Proc. of Int. Conf. on Industrial Electronics & Applications*, pp. 1686–1689, 2010.
